Optical tweezers in interaction with an apertureless probe

Patrick C. Chaumet
Institut Fresnel (UMR 6133), Université Paul Cézanne, Av. Escadrille Normandie-Niemen, F-13397 Marseille Cedex 20, France

Bernard Pouligny
Centre de Recherche Paul Pascal, Avenue A. Schweitzer 33600 Pessac, France

Rumiana Dimova
Max Planck Institute of Colloids and Interfaces, Science Park Golm, 14424 Potsdam, Germany

Nešo Sojic
Groupe NanoSystèmes Analytiques, Institut des Sciences Moléculaires, UMR 5255, CNRS Université Bordeaux 1, France

(Received 10 May 2007; accepted 19 June 2007; published online 27 July 2007)

We study the possibility of transfering a particle held in a far-field optical trap, namely the classical optical tweezers, to a near-field trap, in the form of a tapered metal tip (otherwise called an "apertureless probe"). The paper is theoretical: we compute the electromagnetic fields in both configurations, based on a vectorial nonparaxial representation of the Gaussian laser beam in the waist region. We afterwards use the coupled dipole method to compute the optical force acting on a spherical dielectric particle, in the $0.2-1$ μm range in diameter. We find that either repulsion or attraction of the particle by the metal probe is possible, depending on the beam polarization state, particle size, and curvature radius of the metal tip. Equilibrium states of the particle in contact with the tip, under illumination by the laser beam, are predicted. © *2007 American Institute of Physics*. [DOI: 10.1063/1.2759892]

I. INTRODUCTION

Optical tweezers[1] are now a well-established tool in the arsenal of optical microscopy techniques. Classically, optical trapping is achieved near the focus of a laser beam that has been passed through a very large aperture microscope objective. This configuration allows both observing and manipulating small structures within the microscope field of view. The spatial resolution, being in the context of far-field microscopy, is at best on the order of a visible wavelength (λ).

As is well known, scanning techniques exploiting the near-field components of the electromagnetic (EM) field now allow building images with subwavelength resolution.[2] These techniques usually employ a small aperture or a tapered metal tip (a so-called "apertureless probe"),[3] which is moved very short distance ($\ll\lambda$) above the object to be imaged. Inspired by the recent developments in far-field optical trapping, researchers have looked for the possibility of combining imaging and manipulation modes in optical near-field microscopy.[4–8] For instance, numerical studies by Novotny *et al.*,[4] and Furukawa and Kawata,[8] predicted that enhancement of the EM field near the extremity of a metal tip illuminated by a plane wave is large enough to provide a stable optical trap for nanometer-sized dielectric particles. A similar conclusion was arrived at by Okamoto and Kawata,[5] and Kwak *et al.*[7] with a nanoaperture through a metal surface. An alternate configuration, involving an apertureless metal probe above a dielectric surface illuminated from below in the total internal reflection regime has been investigated by Chaumet *et al.*[6] These authors analyzed and demonstrated the possibility of using the metal tip to pick up and move particles above the substrate, playing with in-plane [transverse magnetic (TM)] and out-of-plane [transverse electric (TE)] polarizations of the illuminating field.

In this article, we study the experimental scheme in which a particle held by optical tweezers can be transferred to a near-field probe, in the form of a metal tip (see Fig. 1). In other words, we address the problem of relaying a far-field optical trap by a near-field one. This theoretical paper is designed as a predictive tool to guide experiments to come. In principle, these experiments will combine classical optical tweezers and a metal tip that will be driven close to the focus of the laser beam. We suppose that a spherical dielectric particle has been stably trapped by the laser beam and investigate the perturbation caused to the particle equilibrium by the proximity of the metal tip (see Fig. 1). Basically, we want to know whether the force between the particle and the metal tip is repulsive or attractive, and whether the particle can be

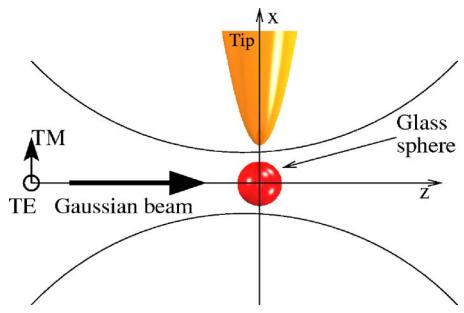

FIG. 1. (Color online) Geometry of the optical manipulation. A Gaussian beam traps a glass particle immersed in water. A tapered metal probe is afterwards brought close to the particle.

kept in stable contact with the tip. Particle sizes are in the 0.2–1 μm range, somehow at the lower limit for observability in real experiments. The paper is organized as follows: in Sec. II, we set out the method to compute EM fields and the related optical forces. We first briefly summarize the principles of the coupled dipole method and pose the relation used for computing optical forces (Sec. II A) in general.[9] As we deal with tightly focused laser beams, it is necessary to go beyond the classical (paraxial) formalism of Gaussian beams to describe the focal region of the beam. This problem is the matter of Sec. II B: based on the angular spectrum representation of Gaussian beams,[10] we set up expressions for the three-dimensional EM field and its derivatives near the focus of the beam, beyond the paraxial approximation. Section III A deals with the primary problem of computing trap forces in the pure optical tweezers geometry, i.e., an isolated spherical particle trapped by a large aperture beam. Axial and lateral trap forces are computed for TE and TM field configurations. We come to the metal-tip problem in Sec. III B. We first consider the perturbation caused by a metal tip approaching a particle held in the trap region of an optical tweezers, and show that the tip–particle interaction may be either attractive or repulsive according to the field polarization. We afterwards consider the situation of a sphere in contact with the tip, in a coaxial configuration, and determine whether this configuration can be kept stable under the sole action of optical forces. These findings are discussed in Sec. IV within the prospect of experimental testing with silica or polystyrene particles in water. We add a discussion about colloidal forces and possible complications due to heating of the metal tip and the resulting convection of the fluid around it. The paper is summarized and concluded in Sec. V. Complete definitions of functions used in Sec. II and for the laser beam power, are given in Appendices A and B, respectively. Estimates of colloidal forces are derived in Appendix C.

II. COMPUTATION OF THE OPTICAL FORCES

A. The coupled dipole method

We use the so-called coupled dipole method (CDM) to compute the optical forces. Below, we only briefly recall the principles of the method, referring the reader to previous publications for details.[9,11] The object under study is represented by a cubic array of N polarizable subunits. The electric local field $\mathbf{E}(\mathbf{r}_i)$ at each subunit position $\mathbf{r}_i$ can be expressed as

$$\mathbf{E}(\mathbf{r}_i) = \mathbf{E}_0(\mathbf{r}_i) + \sum_{j=1}^{N} \mathbf{T}(\mathbf{r}_i,\mathbf{r}_j)\alpha(\mathbf{r}_j)\mathbf{E}(\mathbf{r}_j), \tag{1}$$

where $\mathbf{E}_0(\mathbf{r}_i)$ is the incident field at position $\mathbf{r}_i$. $\mathbf{T}$ is the Green function for the field radiated by a dipole in free space.[12] $\alpha(\mathbf{r}_j)$ is the polarizability of the subunit j, within which we include the Claussius–Mossotti relation for the radiative reaction term.[13] Then, the time-averaged optical force experienced by each subunit is given by

$$F_k(\mathbf{r}_i) = (1/2)\mathrm{Re}\left[\alpha(\mathbf{r}_i)E_l(\mathbf{r}_i)\left(\frac{\partial}{\partial k}E^l(\mathbf{r})\right)^*_{\mathbf{r}=\mathbf{r}_i}\right], \tag{2}$$

where k and l stand for the components along either x, y, or z, Re denotes the real part and $*$ the complex conjugate. Note that the above relation contains both components of the optical force, usually referred to as the "gradient" and "scattering" force components in the basic formulation of optical tweezers theory.[1,14,15] As the object is a set of N small subunits, we obtain the total force on the particle by simply summing the $\mathbf{F}(\mathbf{r}_i)$ contributions on each dipole.

To compute the optical forces one needs the derivative of the local field, which can be obtained in deriving Eq. (1).[16] Computing the local field derivative involves expressions of both the incident field and its derivative: these expressions are set out in Sec. II B, below.

B. Definition of the Gaussian beam

Optical levitation and trapping of micrometer-sized particles has been abundantly demonstrated with Gaussian laser beams.[1] Optical forces due to a single beam have already been computed, based on approximate representations of the EM field, in ray optics or paraxial regimes (for a summary and a list of useful references, see Sec. VI in Ref. 1). For instance, the case of a beam of moderate aperture has been treated through a generalization of the Lorenz–Mie theory,[17–19] or using the T-matrix method.[20] The representation of a tightly focused beam (in other words, of a very large aperture beam), as those used in single-beam optical tweezers designs, is a much more involved problem, which has only been tackled in recent years.[21–25]

The manipulation of a nonabsorbing particle of size on the order of a wavelength is often done with a highly focused beam obtained through a high numerical aperture objective lens, see, for example, Refs. 14, 26, and 27. The laser beam is classically represented as Gaussian.[14,26,27] Below, we set out expressions for a tightly focused beam, whose intensity profile in the beam-waist plane is Gaussian.

When the waist, w_0, is smaller than the wavelength, the beam must be described as vectorial, with both transverse and longitudinal components. The problem of interest in this article, i.e., computing the forces acting on a particle trapped in the focal region of the beam, calls for expressions for the vector EM field in this region. Below, we derive exact expressions, based on the so-called angular spectrum representation of the beam:[10,28]

$$E_x(\mathbf{r}) = \int_{-\infty}^{+\infty}\int_{-\infty}^{+\infty} A_x(k_x,k_y)\exp[i(k_x x + k_y y + k_z z)]\mathrm{d}k_x\mathrm{d}k_y, \tag{3}$$

$$E_y(\mathbf{r}) = \int_{-\infty}^{+\infty}\int_{-\infty}^{+\infty} A_y(k_x,k_y)\exp[i(k_x x + k_y y + k_z z)]\mathrm{d}k_x\mathrm{d}k_y, \tag{4}$$

$$E_z(\mathbf{r}) = -\int_{-\infty}^{+\infty}\int_{-\infty}^{+\infty}\left[\frac{k_x}{k_z}A_x(k_x,k_y) + \frac{k_y}{k_z}A_y(k_x,k_y)\right] \times \exp[i(k_x x + k_y y + k_z z)]\mathrm{d}k_x\mathrm{d}k_y, \quad (5)$$

where the z axis is the direction of propagation. The wave vector has a magnitude k_0, with $k_0^2=k_x^2+k_y^2+k_z^2$. The beam is defined as Gaussian in the $z=0$ plane,[23] i.e., $E_l(x,y,0) = E_{0l}\exp(-\rho^2/2w_0^2)$ with $\rho^2=x^2+y^2$ and E_{0l} the magnitude of the Gaussian beam at the origin (where l stands for either x or y). Then we obtain

$$A_l(k_x,k_y) = E_{0l}\frac{w_0^2}{2\pi}\exp\left(-\frac{k^2 w_0^2}{2}\right), \quad (6)$$

with $k^2=k_x^2+k_y^2$. The above relations are the basis for computing the EM field components everywhere in space.[28] After some algebra (see Ref. 28 for details), we arrive at the following set of exact expressions, for the components of the EM field. We derive analytical expressions for the field derivatives as well, to be used for the computation of the optical forces:

$$E_l(\mathbf{r}) = E_{0l}I_1(\mathbf{r}), \quad (7)$$

$$E_z(\mathbf{r}) = -i(\sin\theta E_{0x} + \cos\theta E_{0y})I_4(\mathbf{r}), \quad (8)$$

$$\frac{\partial E_l(\mathbf{r})}{\partial x} = -E_{0l}I_2\sin\theta, \quad (9)$$

$$\frac{\partial E_l(\mathbf{r})}{\partial y} = -E_{0l}I_2\cos\theta, \quad (10)$$

$$\frac{\partial E_l(\mathbf{r})}{\partial z} = E_{0l}I_3, \quad (11)$$

$$\frac{\partial E_z(\mathbf{r})}{\partial x} = -E_{0x}[\cos(2\theta)I_6 + I_5] + E_{0y}I_6\sin(2\theta), \quad (12)$$

$$\frac{\partial E_z(\mathbf{r})}{\partial y} = E_{0y}[\cos(2\theta)I_6 - I_5] + E_{0x}I_6\sin(2\theta), \quad (13)$$

$$\frac{\partial E_z(\mathbf{r})}{\partial z} = I_2(\sin\theta E_{0x} + \cos\theta E_{0y}), \quad (14)$$

with $\sin\theta=x/\rho$, $\cos\theta=y/\rho$. Definitions of the I_i terms for $i=1,\ldots,6$ are given in Appendix A, in the form of integrals on k.

III. RESULTS

The configuration of interest in this article is sketched in Fig. 1. We assume a Gaussian beam, of waist w_0, at wavelength $\lambda=1060$ nm in vacuum, and of constant power, $P=0.1$ W (the relation between P and the magnitude E_0 of the incident field is given in Appendix B). The focused Gaussian beam provides an optical trap, to be used to manipulate and move a sphere of radius a. We suppose that the particle and the tip are immersed in water ($n_{\text{water}}=1.33$), as in the real experimental situation.

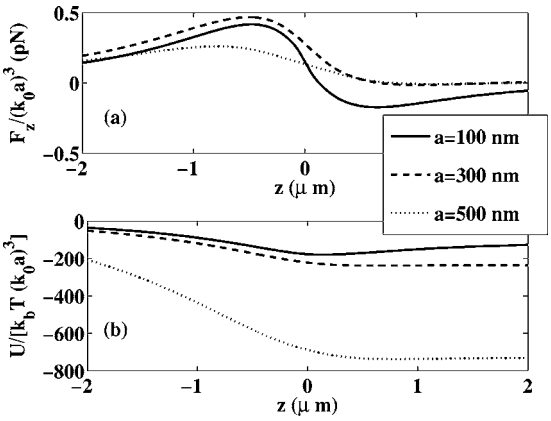

FIG. 2. (a) z component of the force experienced by a glass sphere ($n=1.5$) of radius a embedded in water ($n_{\text{water}}=1.33$), along the z axis, when it is illuminated by a Gaussian beam, with $P=0.1$ W, $w_0=400$ nm $\lambda=1060$ nm in vacuum. For clarity and reference to the Rayleigh approximation, the force is scaled by $(k_0a)^3$. $a=100$ nm in bold line, $a=300$ nm in dashed line and $a=500$ nm in dotted line. (b) Work required to bring the sphere from $z=-\infty$ to z, in k_bT units scaled by $(k_0a)^3$. The position of stable equilibrium corresponds to $z_{\text{equi}}=146$ nm for $a=100$ nm, $z_{\text{equi}}=668$ nm for $a=300$ nm and $z_{\text{equi}}=791$ nm for $a=500$ nm.

A. Isolated particle in a Gaussian beam

Here, we address the situation when the tip is absent, i.e., the ordinary optical tweezers problem, with a spherical particle in water. Figures 2 and 3 show the trapping performance of the configuration for three different values of the particle radius a, in longitudinal and transverse directions, respectively. The particle is supposedly made of glass ($n=1.5$). In Fig. 2(a), F_z is the component of the optical force along the z axis. The beam-waist value is fixed: $w_0=400$ nm. To help the readability of the diagram, the force has been scaled by $(k_0a)^3$. The third power in a was chosen in reference to the Rayleigh regime, corresponding to $a \ll \lambda$: in this limit, optical gradient forces are proportional to a^3. Applicability of the Rayleigh approximation would mean that all curves merge onto a single master curve. Clearly, this is not so, meaning that the particle radii in the examples of Fig. 2 are well above the Rayleigh limit.

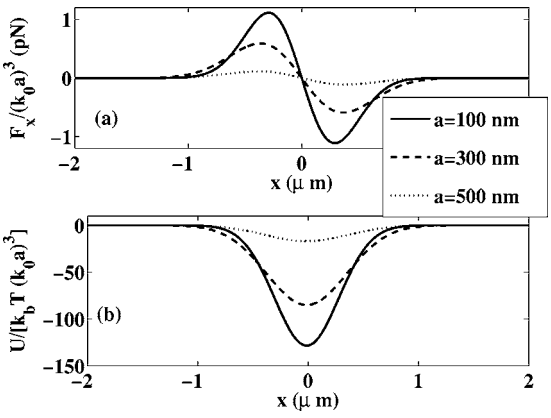

FIG. 3. (a) x component of the optical force scaled by $(k_0a)^3$ (the sphere moves parallel to the x axis, in the plane corresponding to the position of axial stable equilibrium, $z=z_{\text{equi}}$ and $y=0$). $a=100$ nm in bold line, $a=300$ nm in dashed line and $a=500$ nm in dotted line. (b) Work required to bring the sphere from $x=-\infty$ to x, in k_bT ($T=300$ K) units scaled by $(k_0a)^3$.

TABLE I. Depth of the optical trap potential well, versus beam-waist and particle radius. Brownian excursions of the particle, in rms value, are indicated in brackets.

w_0	350 nm	400 nm
$a=100$ nm	$40k_bT$ (48 nm)	$25k_bT$ (78 nm)
$a=300$ nm	$300k_bT$ (14 nm)	$30k_bT$ (21 nm)
$a=500$ nm	$800k_bT$ (12 nm)	$80k_bT$ (17 nm)

Figure 2(b) shows the work U required to bring the sphere from $z=-\infty$ to z. The quantity in ordinate is scaled to $(k_0a)^3$, as for the force, and the thermal energy k_bT has been taken as the unit energy ($T=300$ K is room temperature and $k_b=1.38\times10^{-23}$ J/K is Boltzmann's constant). The position of stable equilibrium, i.e., the minimum in U [which corresponds to $F_z=0$ in Fig. 2(a)], is located at $z_{\text{equi}}=146$ nm for $a=100$ nm. When a increases, the equilibrium position moves to a slightly positive z: qualitatively, this may be understood as the result of the drastic increase of the scattering force (which grows as a^6 in the Rayleigh limit), while the gradient force only increases as a^3 (again, in Rayleigh limit). Positions of stable equilibrium are $z_{\text{equi}}=668$ nm for $a=300$ nm and $z_{\text{equi}}=791$ nm for $a=500$ nm. Because of the temperature bath, the trapped particle undergoes Brownian excursions, whose variance is given by $\langle z^2\rangle = k_bT(\partial^2U/\partial z^2)^{-1}$. Table I gives the depth of the potential well and the amplitude of the excursion in z (square root of the variance) for the previous particle radii and two different values of the beam waist. Note that the potential depths are definitely larger than $10k_bT$ and that the excursions are always less than a particle radius. Large spheres are more tightly trapped than small ones. Not surprisingly, the efficiency of longitudinal trapping is better with a narrower waist.

Notice that if the paraxial approximation is used, i.e., the well-known approximation for the Gaussian beam as it has been expressed in Ref. 29, Eq. (3), then the optical force obtained for the smaller radius ($a=100$ nm) is very close to that from our rigorous approach. However, this is no longer the case when the particle size increases. Not only the magnitude of the optical force is different (by a factor of 2 when $a=500$ nm), but, more dramatically, the paraxial approach predicts no position of axially stable equilibrium for $a=300$ nm and $a=500$ nm. This comparison shows the importance of a rigorous description of the large aperture Gaussian beam structure in computing optical forces.

Figure 3(a) shows the transverse component of the optical force, supposing a beam polarization parallel to the figure plane, (x,z) (from now on, this configuration will be referred to as TM). Figure 3(a) shows the force experienced by the sphere when moving parallel to the x axis, at $y=0$ and $z=z_{\text{equi}}$. Figure 3(b) corresponds to the work required to bring the sphere from $x=-\infty$ to x, taking k_bT as the unit energy, as before. Clearly, the potential well is always larger than $10k_bT$. Therefore we conclude that the spheres are stably trapped in the three spatial dimensions.

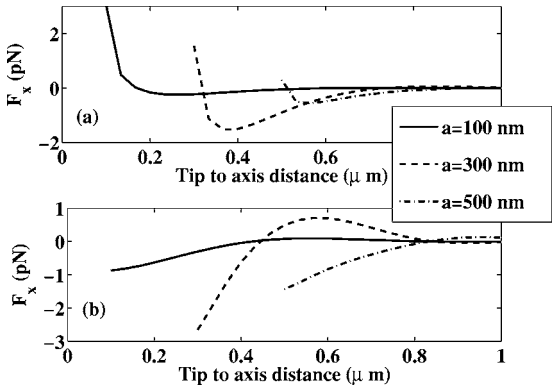

FIG. 4. x component of the optical force experienced by the sphere along the x axis versus tip to axis distance. $r=100$ nm at the tip apex. The sphere is initially located at its position of stable equilibrium. $a=100$ nm in bold line, $a=300$ nm in dashed line, and $a=500$ nm in dotted dashed line. (a) Polarization of the field along the x axis: TM polarization; (b) polarization of the field along the y axis: TE polarization.

We checked that the polarization only induces a very small anisotropy in the transverse force: in other words, switching the polarization from TM to TE hardly changes the x force profile.

B. Particle in presence of a metallic tip

Now we want to study the effects of a metallic probe approaching a sphere trapped by the Gaussian beam. We suppose that the probe is made of tungsten ($n_{\text{W}}=3+3.8i$), and represent its extremity as a portion of a sphere, r in radius. Although the probe may be macroscopic in overall length, the EM field only hardly penetrates inside the metal because of the very strong absorption (the skin depth is about 25 nm),[30] moreover the incident field decreases very quickly versus ρ (with $w_0=400$ nm, the amplitude of the incident field is about $0.05E_0$ for $\rho=950$ nm). Both attenuations simplify the degree of discretization needed in the numerical computation, as we may safely truncate the penetration depth inside the metal to about a wavelength. In this context, the metal probe is simply equivalent to a spherical cap of radius r.

Physically, the influence of the probe on the particle equilibrium is due to light scattering by the metal, which causes a modification of the EM field felt by the particle. Of course, this effect should be important only when the tip gets very close to the particle.

Figure 4 shows the x component of the force experienced by the sphere for a variable tip-to-optical axis distance (d), down to contact with the particle surface, $d=a$. The sphere is supposedly held at its stable equilibrium position in the absence of the metal probe: $x=y=0$ and $z=z_{\text{equi}}$. The symmetry axis of the probe coincides with $y=0$ and $z=z_{\text{equi}}$.

In TE configuration [i.e., far from the beam axis, the electric field is perpendicular to the (x,z) plane], we find that the sphere experiences a negative force [Fig. 4(b)], meaning a repulsion, whenever the metal tip gets close to contact. For $a=300$ nm and $a=500$ nm, Fig. 4(b) shows that the value of the repulsive force is weak, compared to the maximum optical trapping force along the x direction in absence of the tip. In this context, the perturbation caused by the tip is weak.

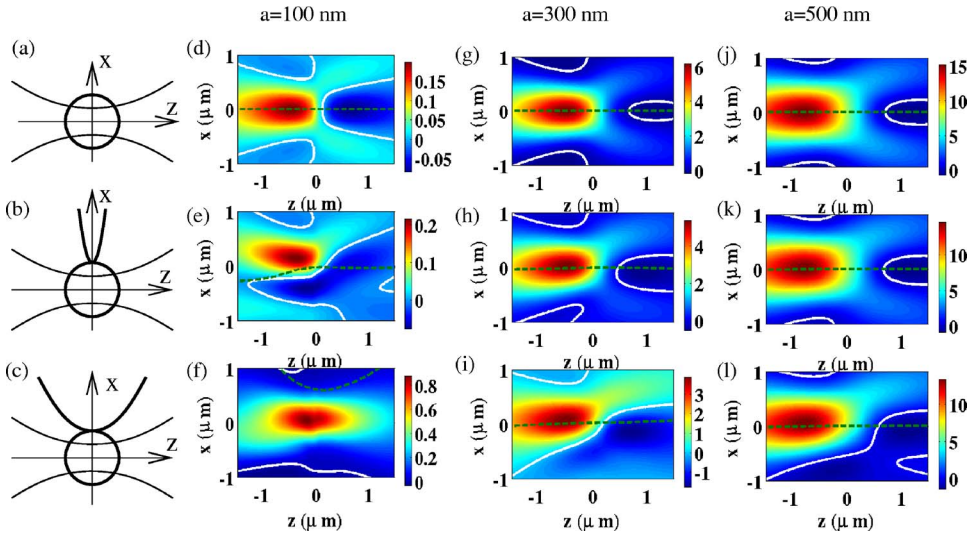

FIG. 5. (Color online) (a) (Without a tip), (b) ($r=10$ nm), and (c) ($r=100$ nm). (d), (e), and (f): $a=100$ nm. (g), (h), and (i): $a=300$ nm. (j), (k), and (l): $a=500$ nm. Each color map represents the z component of the optical force acting on the sphere, in (x,z) plane. $F_z=0$ along the white bold line, and $F_x=0$ along the green dashed line: above this line, $F_x<0$ (sphere–tip repulsion), and below this line, $F_x>0$ (sphere–tip attraction).

Conversely, for the smallest particle size, $a=100$ nm, the repulsion reaches a few pN in amplitude, on the order of the trapping force. Therefore, if only optical forces are present, tip-to-particle contact is impossible in this configuration.

In TM configuration [i.e., far from the beam axis, the magnetic field is perpendicular to the (x,z) plane], the x component of the optical force near contact becomes positive, which means an attractive interaction between the tip and the sphere [Fig. 4(a)]. Physically, the attraction may be understood as being due to the enhancement of the EM field near the tip apex, in TM polarization. As the field enhancement is localized close to the metal surface, the particle feels an increasing field when d decreases, hence, a positive gradient force. Notice that this attractive force decreases when a increases. This is simply due to the lower limitation in the tip-to-laser beam axis distance ($d=a$ at contact), with the consequence that the maximum source field felt by the tip is higher when a is smaller. Note that the force is slightly repulsive when the sphere is 100 nm away from the tip, but the repulsion is too weak to push the sphere outside of the optical trap. When d increases, the optical force quickly vanishes with small oscillations, due to multiple scattering between the tip and the sphere.

In Fig. 4, the tip radius is fixed, $r=100$ nm. If r is decreased down to 10 nm, a similar behavior is obtained but with a smaller value of the force at contact.

We recall that, in the above analysis, the particle was supposedly held fixed at $x=y=0$ and $z=z_{\mathrm{equi}}$, and the probe axis position was set to $y=0$ and $z=z_{\mathrm{equi}}$. We imposed this condition to focus the study on the x component of the particle–metal interaction, in the coaxial configuration, for a particular position of the particle–tip couple along the x axis. Note that an attractive x component of the force is not sufficient to provide particle equilibrium at the metal tip, because the z component of the force, F_z, in general, is not null. We now address the problem of the equilibrium of the particle–tip complex, still in the coaxial configuration (the probe axis goes through particle center), for different positions of the complex inside the (x,z) plane. Equilibrium requires $F_x>0$, $F_z=0$, and $(\partial F_z/\partial z)<0$. Results are displayed in Fig. 5.

The first line of Fig. 5 [Figs. 5(d), 5(g), and 5(j)] shows the situation in the absence of the metal probe, for reference. The field polarization is TM. Figure 5 shows the (color-coded) amplitude of F_z, as a function of x and z, and indicates the sign of the x component: $F_x<0$ ($F_x>0$) above (below), dotted green line, respectively. The line in white shows the case $F_z=0$. In the absence of the probe, Fig. 5 has the symmetry of the laser beam itself, and the dotted line is confounded with the z axis.

The second line, [Figs. 5(e), 5(h), and 5(k)] shows the situation with a very sharp metal probe, corresponding to a very small tip radius ($r=10$ nm). Note that the tip only has a very small influence when the particle is large, i.e., $a\gg r$: the z coordinate of stable equilibrium, z_{equi}, is only slightly decreased [see Fig. 5(h): $a=300$ nm and Fig. 5(k): $a=500$ nm]. Therefore, it should not be difficult to bring the metal tip in contact with the optically trapped particle. The perturbation caused by the tip becomes large with a small particle, $a=100$ nm [see Fig. 5(e)]. The diagram still indicates the existence of a very narrow equilibrium zone, in the form of a small spindle, near the origin. But it may be very difficult to bring the tip–particle complex within this zone, starting from a separated configuration.

Not surprisingly, a less sharp tip has a greater influence ($r=100$ nm), as illustrated in the third line of Fig. 5. Figures 5(i) and 5(l) show that equilibrium is still possible with a large particle ($a=300$ nm and $a=500$ nm, respectively), but with a decreased z_{equi}, as already noticed. However, there is no stable position when the particle is too small, as can be seen from Fig. 5(f) ($a=100$ nm). In this configuration it should be impossible to keep the tip and the sphere in contact.

In summary, we find that the particle–tip complex, in coaxial configuration, can be maintained under the sole action of optical forces, provided that the tip radius is small enough and the particle size large enough. This conclusion holds for a TM polarization of the EM field. Presumably, TE polarization favors dissociation of the complex, whatever

particle and tip sizes. Recall that the computation has been done for a tungsten tip: gold would cause larger interactions, probably with similar but stronger trends.

IV. DISCUSSION

The above calculations led us to conclude that the dielectric sphere can be either brought in contact with or detached from the metal tip through the sole action of optical forces. Up to now, we have only considered the mechanical action of light on the system, and ignored the importance of other interactions, such as Van der Waals, hydration, and electrostatic forces. The latter forces, which we may globally refer to as "colloidal," may in fact be considerable and overwhelm the optical forces in a real experiment. Another matter of complication is light absorption by the metal tip, which inevitably will heat up, with the consequence of a nonuniform temperature distribution over the particle–tip system. The resulting surface temperature gradient will be the source of a fluid convection (the so-called "Maxwellian creep" flow), which through momentum conservation, will impart a force (usually termed "photophoretic") on the system.[31] Estimating the importance of the photophoretic force is a very complex problem by itself, well beyond the scope of this paper. This point will thus remain unanswered, and left as an open question, to be possibly examined in forthcoming experiments. Conversely, orders of magnitude of colloidal forces can be obtained through rather simple statistical thermodynamics, at thermal equilibrium.[32,33] This point is shortly addressed in Appendix C. Our conclusion is that the particles to be used in experiments, because they are electrically charged in water, will inevitably be attracted to the metal tip, and that the related force is expectably considerable (on the order of nanonewtons). However, it is important to realize that this prediction and that about optical forces as well, only holds in the context of equilibrium. The real experimental situation may well be an out-of-equilibrium one, because bringing the particle in contact with the metal implies completely eliminating the fluid film in between, which may last very long on the experimental time scale. Indeed, experiments by Nadal *et al.*, carried out with polystyrene microspheres close to an indium-tin-oxide (ITO) electrode,[34] showed that only a fraction of them would stick on the ITO surface, while the other ones could be trapped and detached by laser radiation pressure forces. At true equilibrium, all of them should have been irreversibly stuck on the conducting surface.

V. CONCLUSION

We have computed the optical forces involved in optical tweezers geometry, based on a rigorous description of the waist region of a tightly focused laser beam. We noticed that details of the beam structure, not accounted for in approximate representations, are important in predicting reverse radiation pressure effects for submicrometer particle sizes. We afterwards studied the perturbation caused by a metal tip approaching the trapped particle, and addressed the question of whether the particle could be kept in stable contact to the tip, under the sole action of optical forces. We found that this was possible, but only for appropriate tip and particle sizes, and laser beam polarization. This positive conclusion is, however, subject to reservation when predicting what will happen in a real experiment: as we commented, colloidal forces, mainly due to electrical charges of glass or polystyrene particles in water, and heating due to metal absorption, may make the actual picture far from that restricted to optical forces only.

ACKNOWLEDGMENTS

This work has been supported by l'Agence Nationale de la Recherche (Programme en Nanosciences et Nanotechnologies ANR-05-NANO-048) and by the French Ministry of Research.

APPENDIX A: INTEGRATION NEEDED TO COMPUTE A GAUSSIAN BEAM

Below, we give explicit expressions for the I_i functions entering Eqs. (7)–(14). Polar coordinates are used for the k variable in the integrals, and k_z is defined by $k_0^2=(\omega/c)^2=k^2+k_z^2$:

$$I_1(\mathbf{r}) = \int_0^{+\infty} w_0^2 f(k)\exp(ik_z z)J_0(k\rho)k\,\mathrm{d}k, \tag{A1}$$

$$I_2(\mathbf{r}) = \int_0^{+\infty} w_0^2 f(k)\exp(ik_z z)J_1(k\rho)k^2\mathrm{d}k, \tag{A2}$$

$$I_3(\mathbf{r}) = i\int_0^{+\infty} w_0^2 f(k)\exp(ik_z z)J_1(k\rho)kk_z\mathrm{d}k, \tag{A3}$$

$$I_4(\mathbf{r}) = \int_0^{+\infty} \frac{k^2 w_0^2}{k_z} f(k)\exp(ik_z z)J_1(k\rho)\mathrm{d}k, \tag{A4}$$

$$I_5(\mathbf{r}) = i\int_0^{+\infty} \frac{w_0^2}{2} f(k)\exp(ik_z z)J_0(k\rho)\frac{k^3}{k_z}\mathrm{d}k, \tag{A5}$$

$$I_6(\mathbf{r}) = i\int_0^{+\infty} \frac{w_0^2}{2} f(k)\exp(ik_z z)J_2(k\rho)\frac{k^3}{k_z}\mathrm{d}k, \tag{A6}$$

where $f(k)=\exp(-k^2w_0^2/2)$, and J_0, J_1, J_2 are the zeroth-, first-, second-order Bessel functions of the first kind, respectively. Notice that we only take into account propagating waves to model the Gaussian beam.[28]

APPENDIX B: POWER OF THE GAUSSIAN BEAM

In this Appendix, we give the relation between the power of the Gaussian beam, P, the field amplitude, $|E_0|$, and the Gaussian beam parameter, k_0w_0. The power is defined as

$$P = \left\langle \iint \mathbf{\Pi}\cdot\mathrm{d}\mathbf{S} \right\rangle, \tag{B1}$$

where $\mathbf{\Pi}=\mathbf{E}\times\mathbf{H}$ is the Poynting vector and $\langle\cdot\rangle$ denotes the time average. Performing the surface integration at the waist ($z=0$) and using Faraday's law, we obtain

$$P = \frac{n\pi c\varepsilon_0}{k_0}|E_0|^2 \int_0^\infty \mathrm{Re}[I_1(I_3+I_5)^*]\rho\, \mathrm{d}\rho, \tag{B2}$$

where $\varepsilon_0 = 8.85\times 10^{-12}$ F/m is the vacuum dielectric constant. After some fastidious computation, we finally obtain the following expression:

$$P = \frac{n\pi c\varepsilon_0 w_0^2}{4}|E_0|^2\left\{1 + \frac{(k_0^2 w_0^2 - 1)\sqrt{\pi}}{2k_0 w_0}\mathrm{Im}[w(k_0 w_0)]\right\}, \tag{B3}$$

where $w(.)$ is the Faddeva function.[35]

APPENDIX C: COLLOIDAL FORCES BETWEEN A DIELECTRIC SPHERE AND A METAL TIP

In this Appendix, we tentatively estimate the amplitudes of colloidal forces between a dielectric sphere, a in radius, and a metal tip. The latter is supposedly equivalent to a metal sphere, r in radius. In the absence of the laser beam, we expect the particle and metal tip to interact through dispersion and electrostatic forces.

Dispersion, otherwise called "Van der Waals" forces, can be estimated through Hamaker's theory. The force between both spherical particles is given by[32,33]

$$F_{\mathrm{VdW}}(h) = \frac{A_{\mathrm{DWM}}}{12h^2}\bar{a}, \tag{C1}$$

with $\bar{a} = 2ar/(a+r)$. In Eq. (C1), h is the closest distance between the surfaces of both bodies, and A_{DWM} is the Hamaker constant for the DWM triplet (denoting as D, W, M the dielectric particle material, water, and metal, respectively). Note that $F_{\mathrm{VdW}}(h)\to\infty$ when $h\to 0$, but the above expression only makes sense in the continuum limit, i.e., on length scales definitely larger than molecular sizes.

A practical estimate of the force at contact is given by Eq. (C1), giving h a cutoff value, between 1 and 2 nm (1.6 nm is standard[33]). The value of A_{DWM} can be measured in dedicated experiments, involving the DWM triplet of interest. Such information is not available to us, but an estimate of A_{DWM} can be obtained combining data for DD, WW, and MM configurations, i.e., triplets in which the intermediate medium is vacuum (or air):

$$A_{\mathrm{DWM}} \approx (\sqrt{A_{\mathrm{DD}}} - \sqrt{A_{\mathrm{WW}}})(\sqrt{A_{\mathrm{MM}}} - \sqrt{A_{\mathrm{WW}}}). \tag{C2}$$

The DD and WW constants have been measured: $A_{\mathrm{DD}} = 66$ zJ for polystyrene, and $A_{\mathrm{WW}} = 37$ zJ, while A_{MM} has been estimated between 100 and 300 zJ, depending on the particular metal.[32] Taking $A_{\mathrm{MM}} = 200$ zJ, we arrive at $A_{\mathrm{DWM}} = 16$ zJ. The latter value, of course, is quite rough, but it is a practical basis in so far as we only need an order of magnitude estimate. Using Eq. (C1), we thus arrive at $F_{\mathrm{Vdw}}(h = 1.6)/\bar{a} \sim 0.5$ pN/nm. With $a = r = 10$ nm, the smallest sizes of interest in this paper, the Van der Waals attraction is on the order of a few piconewtons.

Electrostatic forces will be present in usual experiments involving polystyrene or glass particles in water. In ordinary pH conditions, these particles bear negative surface charges, surrounded by a cloud of positive counterions. The thickness of this cloud is the so-called "Debye length," l_D.[32,33] If such a particle comes close to a conducting surface, say a metal plane, it will "see" its electrostatic image though this plane, which is of the opposite sign. The same is true for the counterions, resulting in an overall attraction of the particle by the metal surface. The energy of the interaction has recently been calculated by Nadal.[36] The force at contact ($h=0$) is finite and given by

$$F_{\mathrm{el}}(h=0) = \frac{2\pi\sigma^2 l_D}{\varepsilon_s\varepsilon_0}a. \tag{C3}$$

In the above expression, σ is the particle surface charge density, and $\varepsilon_s = 80$, the water static relative permittivity. To estimate the electrical attraction, we adopt typical values for the surface charge and Debye length: $\sigma = 1$ electron charge per 10 nm^2 (Ref. 37) and $l_D = 100$ nm. We thus arrive at $F_{\mathrm{el}}(h=0)/a = 200$ pN/nm. This estimation only holds for a particle–metal plane couple, but we may suppose that the result can be generalized to a sphere–metal tip couple, at the expense of replacing a by $\bar{a}$ as in Eq. (C1). The conclusion is that the electrical force is considerably larger than both the Van der Waals and optical forces.

Hydration forces arise due to the presence of hydration shells around the ions located at the interacting surfaces. They are repulsive and the working range is up to about 5 nm. An empirical expression describing them is given by the following equation:

$$F_{\mathrm{h}}(h) = -Kl\exp\left(-\frac{h}{l}\right), \tag{C4}$$

where the characteristic length scale l ranges between 0.6 nm and 1.1 nm, and K depends on the hydration of the surfaces but is generally below 3–30 mJ/m^2. For the limit of $h\to 0$ and taking $l = 1$ nm and $K = 20$ mJ/m^2, we obtain $F_{\mathrm{h}}(h=0) = 2$ pN/m, which is comparable to the Van der Waals force. Hydration forces measured between silica surfaces have been found to reach up to about 10 pN/nm.[33] In any case, the hydration repulsion is negligible as compared to the electrostatic force.

[1] K. C. Neuman and S. M. Block, Rev. Sci. Instrum. **75**, 2787 (2004).
[2] F. de Fornel, *Evanescent Waves, Optical Sciences* (Springer, New York, 2001), Vol. 73.
[3] G. Wurtz, R. Bachelot, and P. Royer, Eur. Phys. J.: Appl. Phys. **5**, 269 (1999).
[4] L. Novotny, R. X. Bian, and X. S. Xie, Phys. Rev. Lett. **79**, 645 (1997).
[5] K. Okamoto and S. Kawata, Phys. Rev. Lett. **83**, 4534 (1999).
[6] P. C. Chaumet, A. Rahmani, and M. Nieto-Vesperinas, Phys. Rev. Lett. **88**, 123601 (2002).
[7] E.-S. Kwak, T.-D. Onuta, D. Amarie, R. Potyrailo, B. Stein, S. C. Jacobson, W. Schaich, and B. Dragnea, J. Phys. Chem. B **108**, 13607 (2004).
[8] H. Furukawa and S. Kawata, Opt. Commun. **148**, 221 (1998).
[9] P. C. Chaumet, A. Rahmani, and M. Nieto-Vesperinas, Phys. Rev. B **66**, 195405 (2002).
[10] L. Mandel and E. Wolf, *Optical Coherence and Quantum Optics* (Cambridge University Press, London, 1995).
[11] P. C. Chaumet, A. Sentenac, and A. Rahmani, Phys. Rev. E **70**, 036606 (2004).
[12] J. D. Jackson, *Classical Electrodynamics*, 2nd ed. (Wiley, New York, 1975).
[13] A. Rahmani, P. C. Chaumet, and G. W. Bryant, Astrophys. J. **607**, 873 (2004).
[14] A. Ashkin, J. M. Dziedzic, J. E. Bjorkholm, and S. Chu, Opt. Lett. **11**, 288 (1986).
[15] P. C. Chaumet and M. Nieto-Vesperinas, Opt. Lett. **25**, 1065 (2000).

[16]P. C. Chaumet, A. Rahmani, A. Sentenac, and G. W. Bryant, Phys. Rev. E **72**, 046708 (2005).
[17]K. F. Ren, G. Gréhan, and G. Gouesbet, Opt. Commun. **108**, 343 (1994).
[18]J. A. Lock, Appl. Opt. **43**, 2532 (2004).
[19]J. A. Lock, Appl. Opt. **43**, 2545 (2004).
[20]T. A. Nieminen, H. Rubinsztein-Dunlop, N. R. Heckenberg, and A. I. Bishop, Comput. Phys. Commun. **142**, 468 (2001).
[21]H. Polaert, G. Gréhan, and G. Gouesbet, Appl. Opt. **37**, 2435 (1998).
[22]C. G. Chen, P. T. Konkola, J. Ferrera, R. K. Heilmann, and M. L. Schattenburg, J. Opt. Soc. Am. A **19**, 404 (2002).
[23]G. P. Agrawal and D. N. Pattanayak, J. Opt. Soc. Am. **69**, 575 (1979).
[24]A. Ciattoni, B. Crosignani, and P. Di PortoChew, Opt. Commun. **202**, 17 (2002).
[25]A. Rohrbach and E. H. K. Stelzer, J. Opt. Soc. Am. A **18**, 839 (2001).
[26]P. Bartlett and S. Henderson, J. Phys.: Condens. Matter **14**, 7757 (2002).
[27]R. C. Gauthier and S. Wallace, J. Opt. Soc. Am. B **12**, 1680 (1995).
[28]P. C. Chaumet, J. Opt. Soc. Am. A **23**, 3197 (2006).
[29]R. R. Agayan, F. Gittes, R. Kopelman, and C. F. Schmidt, Appl. Opt. **41**, 2318 (2002).
[30]M. Born and E. Wolf, *Principles of Optics* (Pergamon, New York, 1959).
[31]A. B. Pluchino and S. Arnold, Opt. Lett. **10**, 261 (1985).
[32]R. J. Hunter, *Foundations of Colloid Science* (Clarendon, Oxford, 1986).
[33]J. Israelashvili, *Intermolecular and Surface Forces*, 2nd ed. (Academic, London, 1992).
[34]F. Nadal, F. Argoul, P. Hanusse, and B. Pouligny, Phys. Rev. E **65**, 061409 (2002).
[35]I. S. Gradshteyn and I. M. Ryzhik, *Table of Integrals, Series and Products, Corrected and Enlarged Edition* (Academic, New York, 1980).
[36]F. Nadal, Ph.D. thesis, Université Bordeaux 1, France (2000).
[37]H. Versmold, U. Wittig, and W. Härtl, J. Phys. Chem. **95**, 9937 (1991).